PHYSICAL REVIEW D **81,** 034026 (2010)

Hard photon production and matrix-element parton-shower merging

Stefan Höche,[1] Steffen Schumann,[2] and Frank Siegert[3,4]

[1]*Institut für Theoretische Physik, Universität Zürich, CH-8057 Zürich, Switzerland*
[2]*Institut für Theoretische Physik, Universität Heidelberg, D-69120, Heidelberg, Germany*
[3]*Institute for Particle Physics Phenomenology, Durham University, Durham DH1 3LE, United Kingdom*
[4]*Department of Physics and Astronomy, University College London, London WC13 6BT, United Kingdom*

(Received 22 December 2009; published 19 February 2010)

We present a Monte Carlo approach to prompt-photon production, where photons and QCD partons are treated democratically. The photon fragmentation function is modeled by an interleaved QCD + QED parton shower. This known technique is improved by including higher-order real-emission matrix elements. To this end, we extend a recently proposed algorithm for merging matrix elements and truncated parton showers. We exemplify the quality of the Monte Carlo predictions by comparing them to measurements of the photon fragmentation function at LEP and to measurements of prompt photon and diphoton production from the Tevatron experiments.

DOI: 10.1103/PhysRevD.81.034026 PACS numbers: 13.85.−t, 13.85.Qk, 13.87.−a, 14.70.Bh

I. INTRODUCTION

The measurement of final states containing photons at large transverse momenta plays a key role in collider experiments. Most prominently, at hadron colliders inclusive diphoton or $diphoton + jet$ signatures are promising channels to search for a light Higgs boson [1]. Signatures with photons might furthermore provide access to physics beyond the standard model like supersymmetry or extra spatial dimensions [2]. Less spectacular but extremely important though, photon + jet final states can be used to determine the absolute energy scale of low-p_T jets [3] and to constrain the gluon distribution inside the beam hadron [4]. The success of the outlined physics menu however strongly depends on our ability to thoroughly understand and accurately simulate such prompt-photon production processes in the context of the standard model.

In the framework of perturbation theory, the mechanism of hard-photon production is twofold. A photon can be well-separated from any other particle in the collision, which makes it possible to describe the reaction with fixed-order matrix elements. The fact that these matrix elements include initial- and/or final-state QCD partons necessitates an all-orders resummation of large logarithmic QCD corrections, which are then absorbed into parton distribution functions (PDFs) and fragmentation functions. Because of its vanishing mass, a photon can also be infinitely close to an initial- or final-state QCD parton. The related singularities in hard matrix elements are absorbed into process-independent photon fragmentation functions [5], describing the transition of a QCD parton into a bunch of hadrons and a not well-separated photon during the process of hadronization. Because of the nonperturbative nature of the hadronization process, parton-to-photon fragmentation functions contain a nonperturbative component and must therefore be determined from experimental data. Their evolution with the factorization scale $\mu_{F,\gamma}$ can however be calculated perturbatively. While the description of hard photons through matrix elements is said to yield the direct component of photon observables, the description by fragmentation functions gives the so-called fragmentation component. Both components are related by factorization and must be combined to obtain a meaningful prediction of QCD-associated photon production.

The standard method to theoretically devise a meaningful prompt-photon cross section is to reflect certain experimental photon-isolation criteria in perturbative calculations. However, one must allow for a minimal hadronic activity in the vicinity of the photon. Only then it can then be ensured that all QCD infrared divergences are properly cancelled. Several such criteria are on disposal, e.g. the cone approach [6,7], the democratic approach [8], and the smooth isolation procedure [9]. For both, single- and diphoton production at hadron colliders, the complete next-to-leading order (NLO) QCD corrections to respective direct and fragmentation components are known [6,10–13]. The parton-level Monte Carlo programs JETPHOX [14] and DIPHOX [15] implement these NLO results numerically and allow the user to choose from different photon-isolation criteria. The NLO corrections to the direct channel $\gamma\gamma + 1$ jet have been calculated in [16]. The results for the loop-induced processes $gg \to \gamma\gamma$ [17] and $gg \to \gamma\gamma g$ [18] are also available. Beyond calculations at fixed order, in the strong coupling, large efforts were spent on the evaluation of soft-gluon emission effects and on the resummation of corresponding large logarithms. Soft-gluon resummation up to next-to-next-to leading logarithmic accuracy is taken into account in the program RESBOS [19]. The analytic result for resumming threshold logarithms was presented in [20], while small-x logarithms have been studied in [21]. Only recently a first study of the prompt-photon process in the framework of Soft-Collinear Effective Theory has been presented [22].

Let us note, that there is a further source of final-state photons, namely, decays of hadrons, such as π^0 or η. However, such nonprompt production processes can to some approximation be separated from the other two experimentally and measurements are usually corrected for these effects. This is the case for all experimental data referenced in this work.

In this publication, we pursue a different strategy of simulating final states including photons. We account for the hard-production process, the QCD evolution of initial- and final-state partons, as well as the transition of QCD partons into hadrons by means of a multipurpose Monte Carlo event generator. In this context, the lowest-order matrix elements for single- and diphoton production supplemented with QCD parton showers correspond to the above mentioned direct component. The fragmentation contribution is modeled by the incorporation of QED effects into the parton shower. In fact, a generic algorithm to treat photon radiation is also given by the approach of Yennie, Frautschi, and Suura [23]. This scheme is particularly suited to compute logarithmic corrections arising from soft photon radiation, where the coherent emission off all QED charges involved in the process plays an important role. In this publication, however, we are primarily interested in the production of hard, well-separated photons. Such emissions need to be treated by an improved algorithm; see, for example, [24]. We therefore choose to simulate photon radiation using a dipolelike QED shower model. This approach only presents a primitive approximation to soft photon effects, but is easily realized and no additional free parameters are introduced in the parton-shower algorithm, cf. [25]. Similar methods are employed in most contemporary shower programs [26]. An apparent advantage is that this method also allows for a direct comparison with experimental data since it yields predictions at the level of the experimentally observed particles. In particular, the parton-to-photon fragmentation functions are explicitly modeled this way. As a consequence, no further corrections accounting for the nonperturbative parton-to-hadron transition need to be applied and again no additional free parameters need to be introduced. This is crucial also for the validation of a separation of nonprompt photons from prompt photons as mentioned above. The *democratic* treatment of partons and photons in this approach combines the direct and the fragmentation component in a very natural way. It is well suited for comparison to experiments, where it is often necessary to study the impact of photon-isolation criteria.

An apparent disadvantage of the approach is that it relies on lowest-order matrix elements only, and correspondingly higher-order QCD corrections are taken into account in the approximation of the parton shower only. We improve on this deficiency by including higher-order real-emission matrix elements. Parton-shower simulations supplemented with multileg matrix elements have become a standard tool for the description of QCD radiation accompanying the production of massive gauge bosons [27] or colored heavy states [28]. In this line, we extend the formalism originally presented in [29] to the case of prompt-photon production. This process, as stated before, introduces the additional complication of a second source of photon production—the fragmentation component—which is not present for massive gauge bosons. While in most cases of W- or Z-boson production, the massive boson is the hardest object in the interaction; the photon is unlikely to play this role in most prompt-photon events. We lay out a formalism that is capable of coping with this situation and allows us to consistently combine tree-level matrix elements of variable photon and QCD parton multiplicity with a combined QCD + QED parton-shower model. Photons and QCD partons are treated fully democratically in this scheme.

The outline of this paper is as follows. In Sec. II, we introduce our method for simulating photon production using a dipolelike parton-shower model. Section III presents the formalism for combining QCD + QED matrix elements of different final-state multiplicity with the parton shower. We also discuss how to efficiently incorporate a given photon-isolation criterion. In Sec. IV, we present the results of our Monte Carlo analysis and discuss the interplay between the direct photon contribution and the fragmentation component in our approach. Finally, Sec. V contains our conclusions.

II. INTERLEAVED QCD + QED PARTON EVOLUTION

In this section, we briefly recall a formalism which is used in our simulations to generate the combined QCD + QED parton evolution. Similar approaches are implemented in most contemporary shower programs [26]. For simplicity of the argument, we focus on pure final-state evolution. Note that any parton-shower algorithm is uniquely defined by three ingredients: The first is the Sudakov form factor, $\Delta_a(\mu^2, Q^2)$, i.e. the probability for a given parton, a, not to radiate another parton between the two evolution scales Q^2 and μ^2. The second is the ordering or evolution variable. While the Sudakov form factor defines the anomalous-dimension matrix, and thereby the functional form of logarithms which are resummed, the evolution variable selects their argument, i.e. it defines a ''direction'' in the phase space, into which the evolution is performed. The third ingredient of a parton-shower model is the method, which is applied in order to reshuffle momenta of already existing partons when one of them goes off-shell to allow for a branching process.

For QCD parton evolution, we choose to employ the parton-shower algorithm of [30], including the ordering variables for initial-state evolution proposed in [29]. This means that the Sudakov form factor for final-state evolution reads

$$\Delta^{\mathrm{QCD}}_{(ij)}(\mu_0^2, Q^2) = \exp\Bigg\{-\int_{\mu_0^2}^{Q^2} \frac{d\mathrm{k}_\perp^2}{\mathrm{k}_\perp^2} \times \int_{\tilde{z}_-}^{\tilde{z}_+} d\tilde{z} \sum_{i,k} \frac{1}{2} \mathcal{K}^{\mathrm{QCD}}_{(ij)i,k}(\tilde{z}, \mathrm{k}_\perp^2)\Bigg\}, \quad (1)$$

where

$$\mathcal{K}^{\mathrm{QCD}}_{(ij)i,k}(\tilde{z}, \mathrm{k}_\perp^2) = \frac{\alpha_s(\mathrm{k}_\perp^2)}{2\pi} J(\mathrm{k}_\perp^2, \tilde{z}) \langle \mathrm{V}^{\mathrm{QCD}}_{(ij)i,k}(\mathrm{k}_\perp^2, \tilde{z}) \rangle \quad \text{and} \quad \tilde{z} = \frac{p_i p_k}{(p_i + p_j) p_k}. \quad (2)$$

The Jacobian factor J and the spin-averaged dipole functions $\langle \mathrm{V} \rangle$ are defined in [30]. The sums run over all possible splitting products i and all possible spectator partons k of the splitting parton (ij). The ordering parameter is the invariant transverse momentum squared

$$\mathrm{k}_\perp^2 = (Q^2 - m_i^2 - m_j^2 - m_k^2) y_{ij,k} \tilde{z}_i (1 - \tilde{z}_i) - (1 - \tilde{z}_i)^2 m_i^2 - \tilde{z}_i^2 m_j^2, \quad (3)$$

where $Q = p_i + p_j + p_k$, $y_{ij,k} = p_i p_j / (p_i p_j + p_j p_k + p_k p_i)$ and m are the parton masses.

Since QCD and QED emissions do not interfere, their corresponding emission probabilities factorize trivially. A combined QCD + QED evolution scheme is thus obtained by employing the combined Sudakov form factor

$$\Delta(\mu_0^2, Q^2) = \Delta^{\mathrm{QCD}}(\mu_0^2, Q^2) \Delta^{\mathrm{QED}}(\mu_0^2, Q^2), \quad (4)$$

where

$$\mathcal{K}^{\mathrm{QED}}_{(ij)i,k}(\tilde{z}, \mathrm{k}_\perp^2) = \frac{\alpha(\mathrm{k}_\perp^2)}{2\pi} J(\mathrm{k}_\perp^2, \tilde{z}) \langle \mathrm{V}^{\mathrm{QED}}_{(ij)i,k}(\mathrm{k}_\perp^2, \tilde{z}) \rangle. \quad (5)$$

Note that we use spin-averaged dipole functions, not only in the QCD, but also in the QED case. One possible improvement of the present algorithm would therefore be to include the spin-dependent splitting kernels. However, in the domain of hard-photon radiation that we are interested in, this can simply be done by employing the full real-emission matrix element instead. No special treatment is therefore necessary in the parton shower.

The functional form of the spin-averaged splitting kernels is largely constrained by the infrared singularity structure of one-loop QCD amplitudes. It is, however, not fixed and one has the freedom to incorporate nonsingular pieces, which can help to improve the predictions of dipole-shower simulations, cf. [31]. Likewise, the construction of the splitting kinematics is largely constrained by the phase-space variables selected in the splitting. It is, however, not fixed and one has one additional degree of freedom, which corresponds to the choice of the angular orientation of the splitter-spectator system with respect to the remaining particles. One of the most prominent criticisms of the new dipolelike parton-shower models is the seemingly unphysical recoil strategy employed in configurations with initial-state splitter and final-state spectator. This strategy is entirely due to a choice for the momentum mapping between leading-order and real-emission kinematics, which was initially proposed in [32]. The transverse momentum of the emitted parton is thereby compensated by the spectator, leaving not only the virtuality of the splitter-spectator system invariant, but also its complete four-momentum. One can easily imagine a different recoil strategy, where the transverse momentum of the emission is instead compensated by the set of all final-state particles. Such an approach was recently suggested in [33] for the case of massless partons. We extend it to the fully massive case in Appendix A and investigate the corresponding effects on the Monte Carlo results in Sec. IV.

It is otherwise straightforward to extend the above algorithm to initial-state showering. The only subtlety in this context arises from the fact that the fully democratic approach pursued here also allows initial-state photon splitting into a quark-antiquark pair, with the quark (antiquark) initiating the hard scattering. In this case, parton distributions which incorporate QED effects are in principle necessitated. Even though such PDF fits exist (e.g. [34]), the corresponding effects on physical observables should be very small, such that the usage of PDF's without QED contribution does not pose a conceptual problem.

An apparent disadvantage of the above algorithm for generating QED emissions using a parton shower is the low efficiency with which isolated photons will be produced. This problem is dealt with in Appendix B, where we introduce a method to enhance the corresponding emission probability, at the price of generating weighted events.

III. MERGING QCD + QED MATRIX ELEMENTS AND TRUNCATED SHOWERS

In this section, we discuss an algorithm for merging tree-level QCD + QED matrix elements and parton showers, based on the method proposed in [29]. We treat photons and QCD partons democratically, i.e. higher-order tree-level matrix elements can be of order $\alpha^n \alpha_s^m$ compared to the leading order. If $n > 0$, they may contribute to an observed hard-photon final state. In this respect, the inclusion of higher-order real corrections corresponds to shifting the simulation of hard-photon production from the parton-shower to the matrix-element domain.

The merging approach presented in [29] is essentially based on replacing the splitting kernels of the parton shower by the appropriate ratio of full tree-level matrix elements in the domain of hard-parton radiation. This domain is identified by simple phase-space slicing. The slicing parameter, the so-called jet criterion, is given in terms of parton momenta p_i, p_j, and p_k as

$$Q_{ij}^2 = 2p_i p_j \min_{k\neq i,j} \frac{2}{C_{i,j}^k + C_{j,i}^k},$$
$$\text{where } C_{i,j}^k = \begin{cases} \frac{p_i p_k}{(p_i+p_k)p_j} - \frac{m_i^2}{2p_i p_j} & \text{if } j = g \\ 1 & \text{else} \end{cases}. \quad (6)$$

For initial-state partons, one considers the splitting process $a \to (aj)j$ instead of $(ij) \to ij$. With the momentum of the combined particle (aj) given by $p_{aj} = p_a - p_j$, one then *defines* $C_{a,j}^k = C_{(aj),j}^k$. The minimum in Eq. (6) is over all possible color partners k of the combined parton (ij). The jet criterion Q_{ij}^2 identifies—to leading-logarithmic accuracy—the most likely splitting in a dipolelike parton cascade leading to the set of final-state momenta $\{p\}$. The phase-space slicing is now implemented by selecting a cut value Q_{cut} and defining the evolution kernels $\mathcal{K}^{\text{ME}}$ and $\mathcal{K}^{\text{PS}}$ for matrix-element and parton-shower domain as

$$\mathcal{K}^{\text{ME}}_{(ij)i,k}(\tilde{z}, \mathrm{k}_\perp^2) = \mathcal{K}_{(ij)i,k}(\tilde{z}, \mathrm{k}_\perp^2)\Theta[Q_{ij}(\tilde{z}, \mathrm{k}_\perp^2) - Q_{\text{cut}}], \quad (7)$$

$$\mathcal{K}^{\text{PS}}_{(ij)i,k}(\tilde{z}, \mathrm{k}_\perp^2) = \mathcal{K}_{(ij)i,k}(\tilde{z}, \mathrm{k}_\perp^2)\Theta[Q_{\text{cut}} - Q_{ij}(\tilde{z}, \mathrm{k}_\perp^2)]. \quad (8)$$

The kernel $\mathcal{K}^{\text{ME}}$ is then replaced by appropriate ratios of tree-level matrix elements up to a given maximum multiplicity. A detailed description of the corresponding algorithm can be found in [29]. It is obvious that the same procedure can be applied to QED emissions, once they are resummed by the parton shower using Eq. (4). It is then in principle possible to define two separate slicing cuts, $Q_{\text{cut}}^{\text{QCD}}$ and $Q_{\text{cut}}^{\text{QED}}$, which account for the merging of QCD and QED tree-level matrix elements with the parton shower, respectively. Within the context of this work, we choose to leave these slicing cuts identical, since the typical ''hardness'' of a hard well-separated final-state photon is similar to the one of a final-state QCD jet.

In prompt photon production processes, we might be confronted with a situation which cannot arise in pure QCD events, namely, that a single, perturbatively produced particle—the photon—is identified out of potentially many particles forming a broad jet. Several methods exist to achieve this identification. In the democratic approach [8], final-state particles are clustered into jets, treating photons and hadrons equally. The obtained object is called a photon or a photon jet, if the energy fraction $z = E_\gamma/(E_\gamma + E_{\text{had}})$ of an observed photon inside the jet is larger than an experimentally defined value z_{cut}. In the cone approach [6,7], photons are required to have a minimum transverse momentum and to be isolated from any significant hadronic activity within a cone in η-ϕ space. Minimal hadronic activity in the vicinity of the photon (adding of the order of a few GeV to the total transverse momentum in the cone) must thereby be admitted to ensure the infrared finiteness of observables.

While the jet criterion Eq. (6) works very well also for photons defined by the democratic approach, in the case of the cone approach it might not be appropriate to separate matrix-element and parton-shower domain. Note that the main idea of the merging procedure is to improve the parton-shower prediction with fixed-order matrix elements in those regions of phase space which are relevant for the analysis of multijet (multiphoton) topologies. In this respect, it is certainly desirable that experimental requirements are reflected by Q_{ij}^2. This is possible, because the jet criterion, Eq. (6), is not fixed, but rather chosen conveniently to reflect the singularity structure of next-to-leading order real-emission amplitudes in QCD [29]. Moreover, it is a flavor-dependent measure, which allows us to redefine it just for branching processes involving photons. The most common experimental requirements of a minimum transverse momentum and an isolation cone in η-ϕ space could, for example, be reflected by

$$Q_{ij}^2 = \min\{p_{\perp,i}^2, p_{\perp,j}^2\}\frac{\Delta\eta_{ij}^2 + \Delta\phi_{ij}^2}{D^2} \quad \text{and} \quad Q_{ib}^2 = p_{\perp,i}^2, \quad (9)$$

where the first equation applies to final-state photons and charged final-state particles, while the second applies to photons and charged beams. Note that Eq. (9) is essentially equivalent to a longitudinally invariant jet measure [35]. One can now increase the ratio of photons produced through matrix elements over photons produced in the shower by simply lowering the value of $Q_{\text{cut}}^{\text{QED}}$. A convenient way to obtain the largest fraction of events from hard matrix elements is to require a jet separation below the experimental cut on the photon transverse momentum and by setting D lower than the radius of the experimentally imposed isolation cone.

IV. RESULTS

In this section, we apply the event-generation techniques introduced above to prompt-photon production at lepton and hadron colliders. In Sec. IV A, we study the capability of our proposed QCD + QED shower algorithm to reproduce the scale-dependent photon fragmentation function measured in hadronic Z^0 decays at LEP. In Sec. IV B and IV C, we turn the discussion on single- and diphoton final states at hadron colliders, respectively. Besides quantifying the size of the different core-process components in the democratic shower approach, we elaborate on the impact of real-emission matrix-element corrections incorporated using the formalism described in Sec. III. All results presented here are obtained using the Monte Carlo event generator SHERPA [36] in a setup described in Appendix C.

A. The photon fragmentation function

A crucial benchmark for the combined QCD + QED shower algorithm introduced in Sec. II is posed by the

requirement to reproduce the scale-dependent photon fragmentation function $D_\gamma(z_\gamma, y_{\text{cut}})$ [8], where z_γ is the photon's energy fraction with respect to its containing jet and y_{cut} a resolution scale, given e.g. in the Durham scheme. This observable was measured to very high precision in hadronic Z^0 decays by the ALEPH Collaboration [37]. In this analysis, events are selected where all final-state particles are democratically taken into account for jet finding. The events are subdivided into 2-jet, 3-jet and $\geq$ 4-jet topologies with at least one reconstructed jet containing a photon where the photon carries at least 70% of the jet energy ($z_\gamma > 0.7$) and $E_\gamma > 5$ GeV. The resolution measure y_{cut} is varied between 0.01 and 0.33. The measured data is statistically corrected for residual hadronic decay backgrounds and initial-state radiation off the incoming leptons.

Figure 1 shows a comparison between our hadron-level Monte Carlo results and the data from [37]. In the left column, the z_γ distribution for 2-jet events at four different y_{cut} values, namely, 0.01, 0.06, 0.1, and 0.33, are shown. The right column shows corresponding results for 3-jet events at $y_{\text{cut}} = 0.01, 0.06, 0.1$, and $\geq$ 4-jet events at $y_{\text{cut}} = 0.01$. For all the data, $z_\gamma = 1$ corresponds to completely isolated photons, which is reflected by a strong peak in the z_γ distribution. At the parton level, the lowest-order contribution to fully isolated photon production corresponds to $q\bar{q}\gamma$ final states where the quarks form one jet and the photon makes up the other one. At the hadron level, however, this sharp peak gets somewhat broadened by hadronization effects due to the association of soft hadrons with the photon by the jet-clustering algorithm. Our Monte Carlo simulation agrees very well with the data for the measured z_γ range in the three topology classes at the given jet resolutions. This can be seen as a strong indication that the proposed QCD + QED shower scheme is indeed appropriate to describe hard-photon radiation.

The above analysis is especially tailored to study the fragmentation component of the prompt photon production mechanism. The key point in this respect is the application of a democratic jet-clustering procedure which is in one-to-one correspondence with the democratic approach used to compute the photon production rate from the theory in [8]. It is therefore not obvious, that the democratic approach, also underlying our simulation, performs well in experimental situations where the photon must pass a strict isolation criterion, as discussed in Sec. III. We will now turn to investigate such isolated photon final states in more detail, focusing on their emergence at hadron colliders.

B. Prompt-photon hadroproduction

The inclusive production of isolated photons has been measured over a wide range of photon transverse energies by the CDF and D0 experiments at the Fermilab Tevatron at $\sqrt{s} = 1.96$ GeV. In [38], CDF has presented a measurement covering $|\eta_\gamma| < 1.0$ and transverse energies between $30 < E_{T,\gamma} < 400$ GeV. The photon-isolation criterion used corresponds to the requirement that the additional transverse energy found in a cone of $R = \sqrt{(\Delta\phi)^2 + (\Delta\eta)^2} = 0.4$ around the photon is less than 2 GeV. A similar D0 measurement was described in [39]. It covers photons of transverse momentum $p_{T,\gamma} > 23$ GeV up to $p_{T,\gamma} = 300$ GeV and $|\eta_\gamma| < 0.9$. Photon isolation is implemented by demanding $(E_{R=0.4} - E_{R=0.2})/E_{R=0.2} < 0.1$, where E_R is the total energy found in a cone of size R around the photon. Both measurements have been corrected to particle level and the dominant background of photon production from hadron decays, such as $\pi^0 \to \gamma\gamma$ and $\eta \to \gamma\gamma$, has been subtracted. We therefore attempt a comparison with Monte Carlo predictions at the parton level after jet evolution.

Figure 2 compares the data for $d^2\sigma/(dE_{T,\gamma}d\eta_\gamma)$ from [38], respectively, $d^2\sigma/(dp_{T,\gamma}d\eta_\gamma)$ from [39], to our parton-level Monte Carlo results, obtained using leading-order matrix elements in the democratic approach combined with QCD + QED shower evolution. In addition to the total result (red histograms), we display contributions from the different classes of partonic core processes, i.e. from dijet production ($jj \to jj$), single-photon production ($jj \to \gamma j$), and diphoton production ($jj \to \gamma\gamma$). Taking into account the uncertainties of the measurements and the finite Monte Carlo statistics in the high-$E_{T,\gamma}$ bins, our calculation agrees well with the data. For the CDF measurement, the data has a somewhat steeper slope at low $E_{T,\gamma}$ and the Monte Carlo calculation pronounces the high $E_{T,\gamma}$ end of the spectrum. Regarding the different sources of final-state photons in our theoretical model, the main contribution to this observable stems from single photon production. But even though strict isolation criteria are applied, there is a considerable fraction of dijet events, where a hard, isolated photon is produced during the parton-shower evolution in both data samples. This substantiates the argument that the combined shower scheme is crucial for a proper description of such photon final states. The diphoton core process on the other hand is negligible here.

We now turn to study the impact of higher-order real-emission matrix elements on the results. Therefore, we supplement the pure parton-shower evolution by tree-level matrix elements with up to two additional light QCD partons or photons using the matrix-element parton-shower merging formalism described in Sec. III. The comparison with measurements from CDF and D0 is shown in Fig. 3. Besides the total results (red histograms), we again present the subcontributions assigned to matrix-element core processes with exclusively 0, 1, and 2 photons plus a variable number of additional QCD partons. When comparing to Fig. 2, where the pure shower result is shown, it is apparent that the majority of events with a dijet core process in the shower simulation is now ascribed to matrix-element cores with one or two photons plus additional QCD partons.

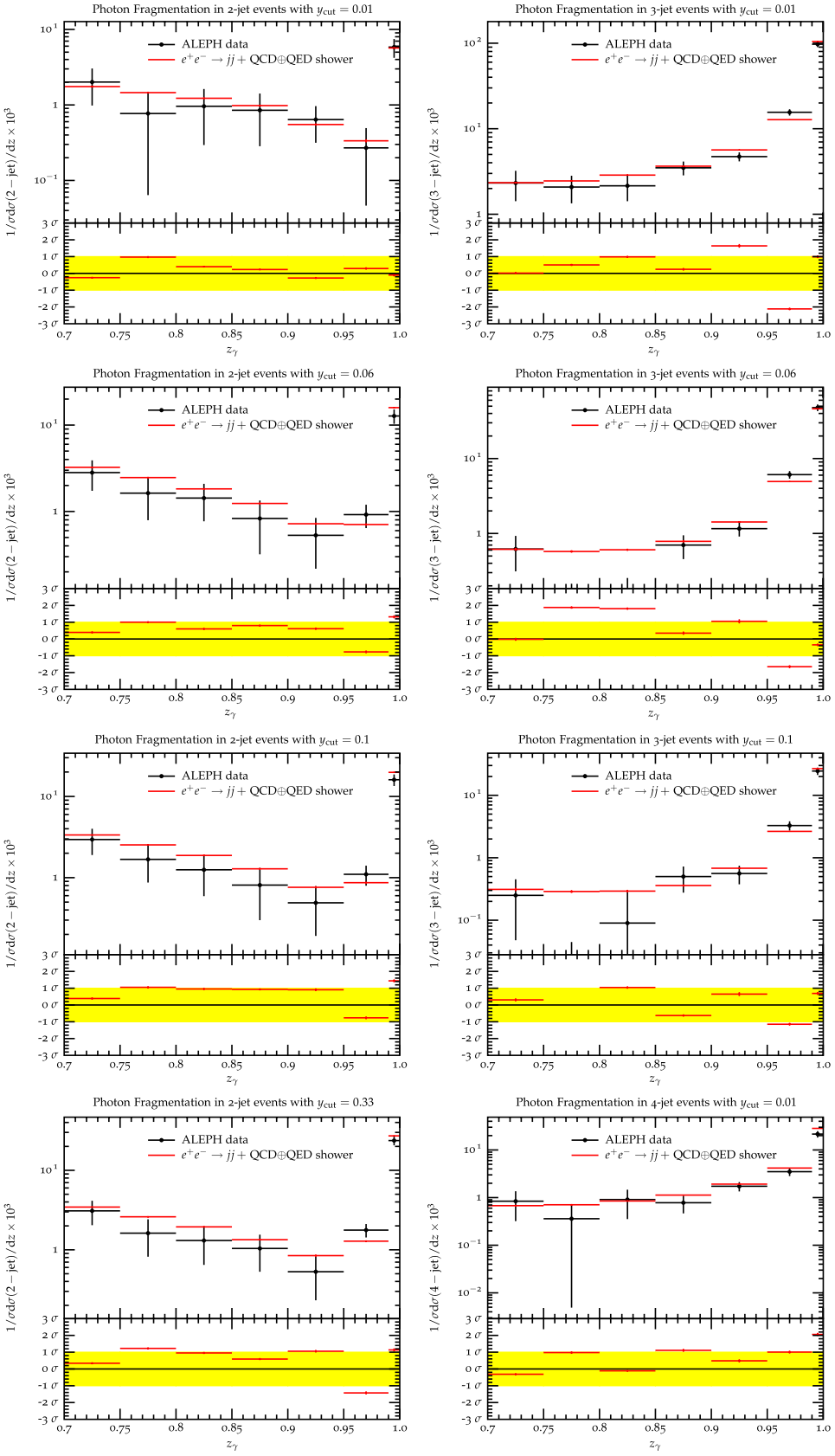

FIG. 1 (color online). The z_γ distribution measured in hadronic Z^0 decays by ALEPH [37] for 2-jet, 3-jet, and $\geq$ 4-jet events at different Durham resolution $y_{\rm cut}$. The theory result corresponds to QCD + QED shower evolution of the leading-order $q\bar{q}$ process, taking into account hadronization corrections.

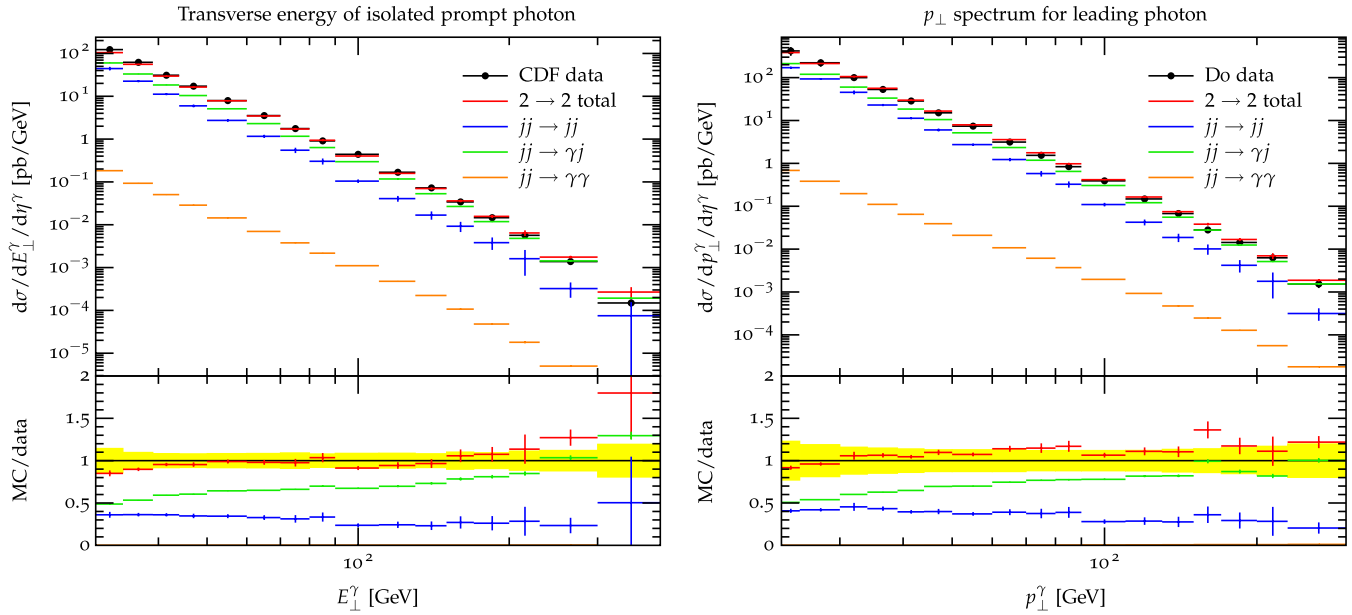

FIG. 2 (color online). Inclusive photon transverse energy distribution compared to data from CDF [38] (left) and D0 [39] (right). The contributions of different classes of leading-order core processes are also displayed. For the notation used cf. the main text.

Thereby, what might traditionally be called *fragmentation* component gets significantly reduced and turned into what is called *direct* component. For this very inclusive measurement, we observe no strong variation of the total result due to the inclusion of real-emission matrix elements. The biggest effect is a somewhat larger inclusive rate for the merged samples $\lesssim 20\%$. The shape of the distributions is preserved. This in fact has to be understood as a highly nontrivial consistency check of our merging formalism.

C. Prompt-diphoton production

An interesting further test bed for the democratic merging approach is diphoton production at hadron colliders. The CDF collaboration has measured properties of the

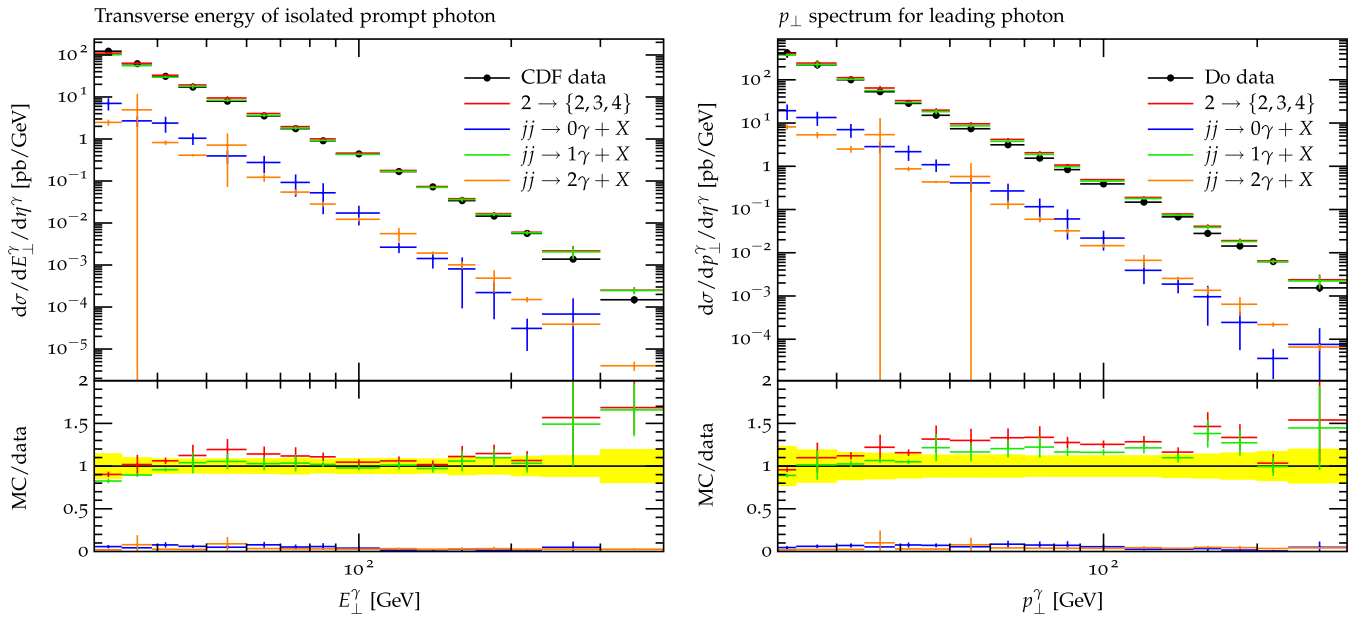

FIG. 3 (color online). The inclusive photon transverse energy obtained with a QCD + QED shower simulation supplemented by real-emission matrix elements with up to two additional QCD partons or photons (denoted $2 \to 2, 3, 4$) is compared to data from CDF [38] (left) and D0 [39] (right).

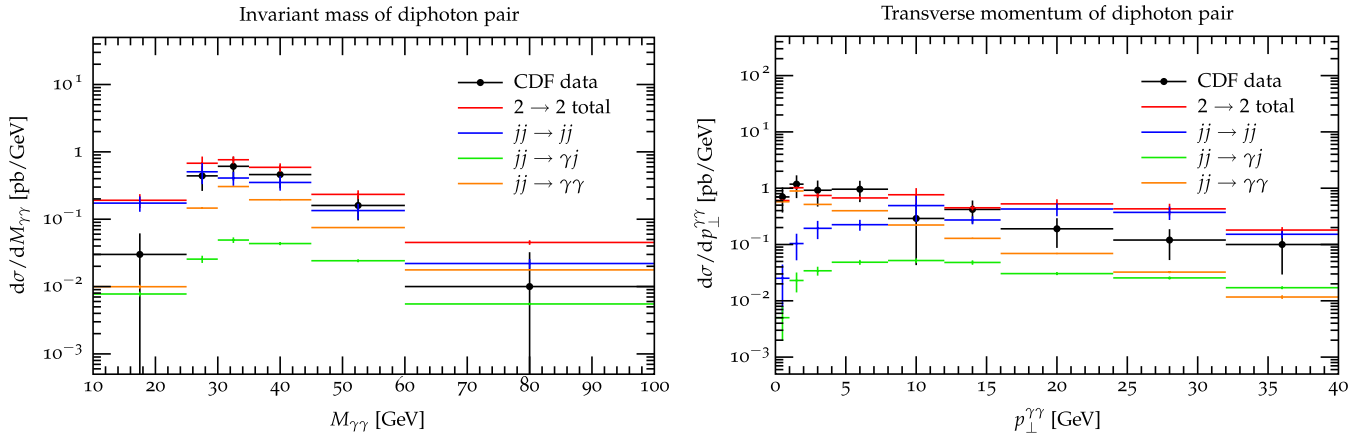

FIG. 4 (color online). Properties of diphoton events measured by CDF [40]. Displayed are the subcontributions from different leading-order matrix elements and their sum.

corresponding final states in some detail. The analysis presented in [40] selects leading/subleading photons with transverse momenta larger than 14/13 GeV. Those must be isolated from any significant hadronic activity within a distance of $R = 0.4$, by requiring the hadronic activity within this cone to yield $E_T < 1$ GeV. For the selected events, the invariant mass and transverse momentum of the photon pair are analyzed as well as the azimuthal separation between the photons.

It is worth noting that our Monte Carlo simulations include the loop-induced contribution $gg \to \gamma\gamma$. It has been shown [40] that its main influence is seen in the invariant mass spectrum around 30 GeV where it accounts for a significant enhancement of the cross section.

To again exemplify the importance of the fragmentation contribution even for the required isolated photons in this analysis, Fig. 4 compares our Monte Carlo prediction for leading-order matrix elements plus shower evolution. It displays the contributions from the previously introduced classes of matrix elements (i.e. $jj \to jj$, $jj \to \gamma j$ and $jj \to \gamma\gamma$). It is evident that the democratic treatment of photons and QCD partons is absolutely mandatory to describe these observables.

From a theoretical perspective, this reaction is interesting because the diphoton system does not have a transverse momentum when described by leading-order matrix elements. Hence, its transverse-momentum spectrum depends strongly on the proper inclusion of higher-order effects. In addition, the azimuthal angle gives a measure for the correlation of the two photons which is also sensitive to higher-order corrections. Especially in the region of large transverse momenta or large decorrelation, one expects these corrections to be better described by matrix elements than by the parton shower.

In this context, the parton-shower kinematics might become important, because the recoil scheme discussed in Sec. II plays an important role for the generation of transverse momentum for the diphoton system. Thus, as a first step, Fig. 5(a) compares parton-level Monte Carlo predictions using two different splitting kinematics. We observe that both the algorithm outlined in Appendix A, denoted "Scheme 1," and the method proposed in [30], denoted "Scheme 2," have difficulties describing the critical regions mentioned above.

We show in Fig. 5(b) that with the inclusion of higher-order real-emission matrix elements, the simulation is able to describe the measurement significantly better. Especially, the transverse-momentum distribution exemplifies two unique features: The resummation of large logarithms correctly reproduces the Sudakov shape of the low-$p_\perp$ region which is not possible with fixed-order calculations. At the same time exact matrix elements allow for a consistent simulation of the high-$p_\perp$ tail where a traditional parton-shower approach would fail. Also, the decorrelation between the photons is now matched very well.[1] The simulation becomes largely independent of the precise implementation of the parton-shower kinematics, an effect which is also observed in [31]. This happens because in the relevant part of the phase space, hard matrix elements are employed to define the kinematics of the diphoton system. In this way, the merging algorithm of Sec. III can be used to eliminate theoretical uncertainties in the parton-shower model employed. At the same time, we substantiate our introductory statement, that within the domain of hard-photon production the parton shower can easily be corrected using higher-order matrix elements.

[1]The deviations in the second and third bin might be due to large statistical fluctuations in the measurement and seem to be contradicted by an earlier albeit unfortunately unpublished D0 measurement [41].

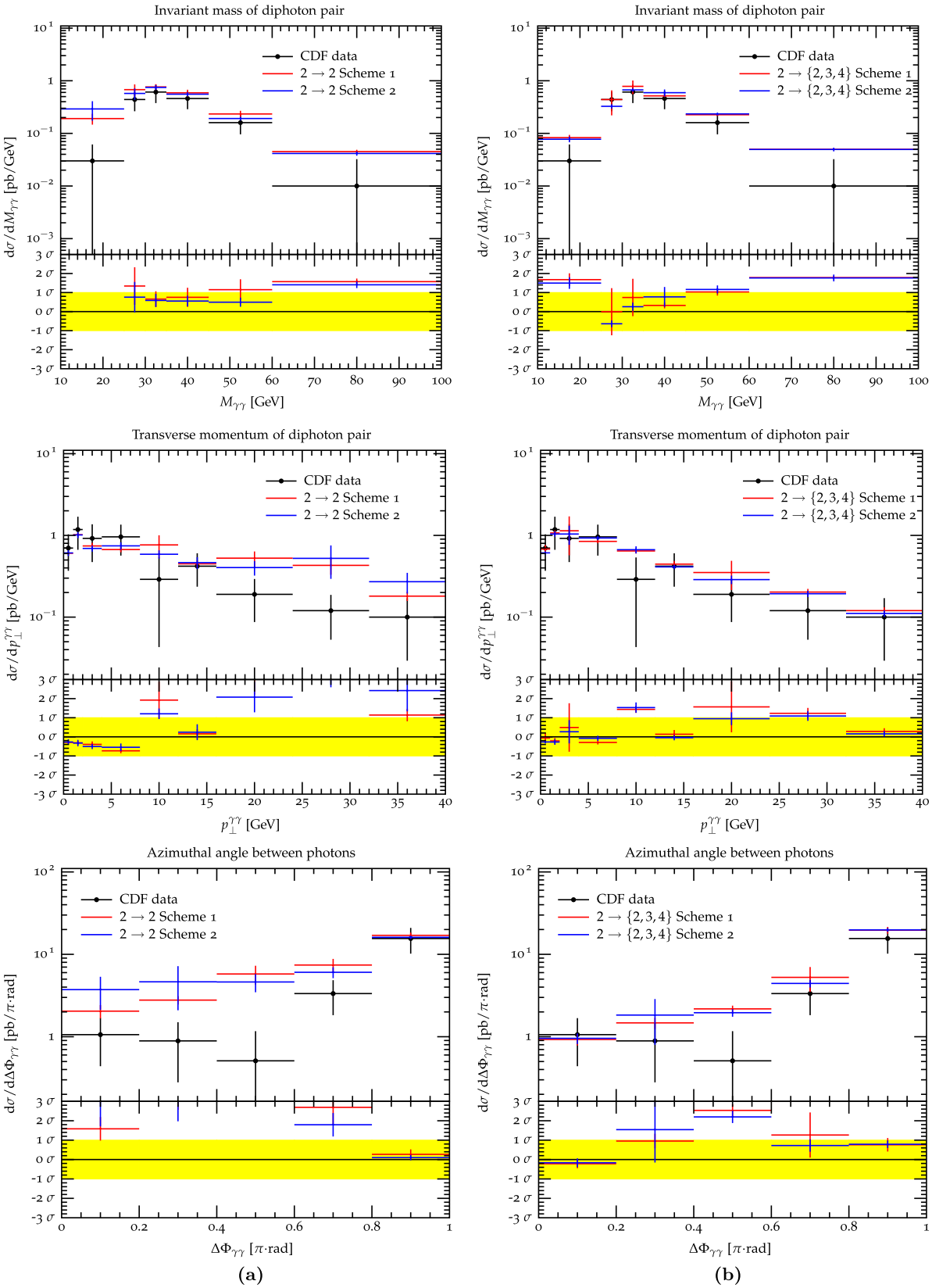

FIG. 5 (color online). Properties of diphoton events measured by the CDF collaboration [40]. Figure (a) compares the influence of different parton-shower kinematics when using leading-order matrix elements. Figure (b) shows the same comparison for merged event samples with up to two additional particles in the matrix element-final state. Scheme 1 refers to the algorithm outlined in Appendix A; scheme 2 stands for the original implementation [30].

V. CONCLUSIONS

We have presented Monte Carlo algorithms for the precise simulation of hard-photon production in collider experiments. Using interleaved QCD + QED evolution in a dipolelike parton shower enables us to simulate the photon fragmentation function within a general-purpose Monte Carlo event generator. Comparison with data from the ALEPH experiment exemplifies the quality of the approach.

To diminish intrinsic uncertainties of parton-shower models, we have supplemented our simulation with higher-order tree-level matrix elements. To do so, an existing algorithm for QCD has been extended to include QED democratically. This can be seen as a first step towards a unified prescription for treating strong and electroweak radiative corrections. At the same time, it provides a natural way to simulate hard-photon production, where the fragmentation component is described consistently by the combined QCD + QED resummation in the parton shower supplemented with a nonperturbative hadronization model. We have employed this procedure to analyze prompt-photon production in hadron-hadron collisions and to find an improved description of Tevatron measurements. Because of a much larger phase space available for radiative corrections, these effects should become even more pronounced at LHC energies.

ACKNOWLEDGMENTS

We would like to thank Thomas Binoth, Gudrun Heinrich, Thomas Gehrmann, and Frank Krauss for numerous fruitful discussions. Help from Thomas Binoth with the code for $gg \to \gamma\gamma$ is gratefully acknowledged. We are grateful to Frank Krauss and Thomas Gehrmann for valuable comments on the manuscript. We also thank Dmitry Bandurin and Michael Begel for their clarifications about the D0 measurement. F. S. would like to thank the ITP Zürich for its hospitality while this work was finalized. S. H. acknowledges funding by the Swiss National Science Foundation (SNF, Contract No. 200020-126691) and by the University of Zürich (Forschungskredit No. 57183003). The work of F. S. was supported by the MCnet Marie Curie Research Training Network (Contract No. MRTN-CT-2006-035606). S. S. acknowledges financial support by BMBF.

APPENDIX A: DIPOLE-SPLITTING KINEMATICS

In this appendix, we derive alternative splitting kinematics for dipolelike parton showers in the spirit of [30]. In addition to the massless case proposed in [33], we give explicit formulas for the fully massive case, which plays an important role for truncated-shower algorithms and in processes involving heavy quarks [42]. Effectively, only one dipole configuration is considered, i.e. branching final-state partons with the spectator parton being in the final state. In this case, we closely follow the proposal in [30], which is inspired by the original kinematics of the massive Catani-Seymour dipoles [32]. Kinematic relations for all other dipole configurations are then derived using crossing relations.

We consider the process depicted in Fig. 6, where a parton $\tilde{ij}$, accompanied by a spectator parton $\tilde{k}$, splits into partons i and j, with the recoil absorbed by the spectator k. We define the combined momenta $p_{ij} = p_i + p_j$ and $Q = p_{ij} + p_k$ and the variables

$$\eta_{ij,k} = \frac{p_i p_j}{p_{ij} p_k}, \qquad \xi_{i,jk} = \frac{p_i p_k}{p_{ij} p_k}. \tag{A1}$$

Thus, we immediately obtain

$$s_{ij} = \frac{\eta_{ij,k}}{1 + \eta_{ij,k}} (Q^2 - m_k^2) + \frac{1}{1 + \eta_{ij,k}} (m_i^2 + m_j^2). \tag{A2}$$

Now let the lightlike helper vectors l and n be given by (cf. [43])

$$l = \frac{p_{ij} - \alpha_{ij} p_k}{1 - \alpha_{ij}\alpha_k}, \qquad n = \frac{p_k - \alpha_k p_{ij}}{1 - \alpha_{ij}\alpha_k}, \tag{A3}$$

where

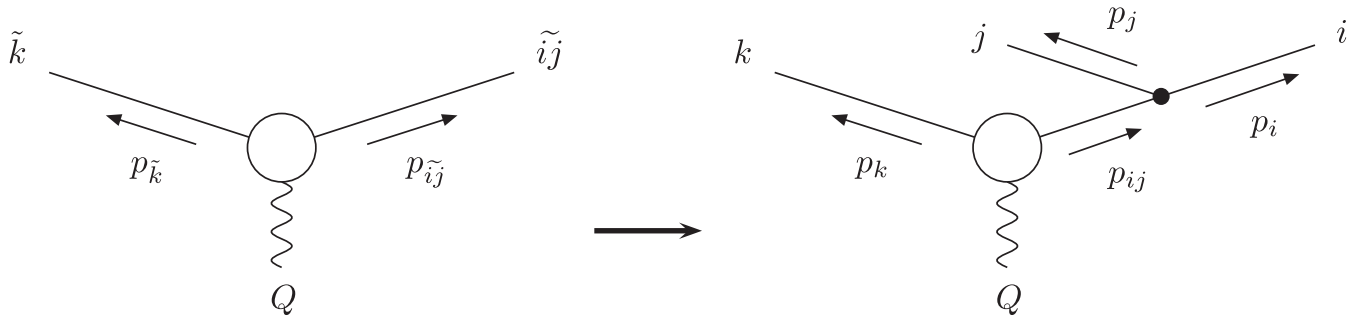

FIG. 6. Schematic view of the splitting of a final-state parton with a final-state spectator. The blob denotes the hard process from which the three partons emerge. Since the four-momentum of the splitter-spectator system is conserved, the pair can be regarded as decay products in a two-particle transition of a virtual particle with momentum $Q = p_{ij} + p_k$.

$$\alpha = \frac{p^2}{\gamma_{ij,k}} \quad \text{and}$$

$$\gamma_{ij,k} = 2\ln = \frac{1}{2}[(Q^2 - s_{ij} - m_k^2) + \mathrm{sgn}(Q^2 - s_{ij} - m_k^2)\sqrt{\lambda(Q^2, s_{ij}, m_k^2)}], \quad \text{(A4)}$$

with λ denoting the Källen function $\lambda(a, b, c) = (a - b - c)^2 - 4bc$.

The momenta p_i and p_j can then be expressed in terms of l, n, and a transverse component $k_\perp$ as

$$p_i^\mu = z_i l^\mu + \frac{m_i^2 + \mathrm{k}_\perp^2}{z_i}\frac{n^\mu}{2ln} + k_\perp^\mu,$$
$$p_j^\mu = (1 - z_i) l^\mu + \frac{m_j^2 + \mathrm{k}_\perp^2}{1 - z_i}\frac{n^\mu}{2\ln} - k_\perp^\mu. \quad \text{(A5)}$$

The parameters z_i and $\mathrm{k}_\perp^2$ of this decomposition are given by

$$z_i = \frac{Q^2 - s_{ij} - m_k^2}{\sqrt{\lambda(Q^2, s_{ij}, m_k^2)}} \times \left[\xi_{i,jk} - \frac{m_k^2}{|\gamma_{ij,k}|}\left(\eta_{ij,k} + \frac{2m_i^2}{Q^2 - s_{ij} - m_k^2}\right)\right],$$
$$\mathrm{k}_\perp^2 = (Q^2 - m_i^2 - m_j^2 - m_k^2)\frac{\eta_{ij,k}}{1 + \eta_{ij,k}} z_i(1 - z_i) - (1 - z_i)^2 m_i^2 - z_i^2 m_j^2. \quad \text{(A6)}$$

Equations (A2) and (A6) are valid for all dipole configurations, i.e. initial and final-state branchings with the recoil partner being either in the initial or in the final state. The corresponding mapping of variables $\eta_{ij,k}$ and $\xi_{i,jk}$ onto those defined for massless partons in [32] is listed in Table I. Note, that in the massless case these kinematic relations reproduce the results of [33].

Constructing a shower emission proceeds as follows:

(1) Determine $\eta_{ij,k}$ and $\xi_{i,jk}$ from evolution and splitting variable.
Compute s_{ij} according to Eq. (A2) and z_i and $\mathrm{k}_\perp^2$ according to Eq. (A6).

(2) Construct p_k according to[2] [32]

$$p_k = \left(\tilde{p}_k - \frac{Q^2 + m_k^2 - m_{ij}^2}{2Q^2} Q\right)\sqrt{\frac{\lambda(Q^2, s_{ij}, m_k^2)}{\lambda(Q^2, m_{ij}^2, m_k^2)}} + \frac{Q^2 + m_k^2 - s_{ij}}{2Q^2} Q. \quad \text{(A7)}$$

(3) From p_{ij} and p_k, construct the lightlike momenta l and n according to Eq. (A3).

[2]Relation (A7) is crossing invariant and can therefore be employed for all dipole configurations.

TABLE I. Mapping of variables for Eqs. (A2) and (A6).

Configuration	$\xi_{i,jk}$	$\eta_{ij,k}$
Final-final	$\tilde{z}_i$	$\frac{y_{ij,k}}{1-y_{ij,k}}$
Final-initial	$-\tilde{z}_i$	$x_{ij,a} - 1$

Configuration	$\xi_{j,ak}$	$\eta_{ja,k}$
Initial-final	$\lvert 1 - \frac{1-u_j}{x_{jk,a}-u_j}\rvert$	$\frac{u_j}{x_{jk,a}-u_j}$
Initial-initial	$1 - \frac{1}{x_{j,ab}+\tilde{v}_j}$	$\frac{-\tilde{v}_j}{x_{j,ab}+\tilde{v}_j}$

Determine the new momenta p_i and p_j according to Eq. (A5).

Because of the possibly vanishing denominator of $\xi_{i,jk}$ and $\eta_{ij,k}$ in the case of initial-state splitters with final-state spectator, the corresponding kinematic relations occasionally become numerically unstable. Except for a tiny region of the phase space, where $|x_{ik,a} - u_i| < \epsilon$, such configurations can be dealt with in the following way: Instead of constructing p_i, we construct $(x_{ik,a} - u_i)p_i$. The energy of this helper momentum is determined using the on-shell constraint for p_i and the whole four-vector is then rescaled with $1/(x_{ik,a} - u_i)$. We typically have ϵ of the order of 10^{-3}.

APPENDIX B: ENHANCING PHOTON PRODUCTION IN THE PARTON SHOWER

To improve the statistical significance of event samples with identified photons described by the parton shower, it is useful to enhance the corresponding branching probabilities. When doing so, one must of course correct for this enhancement by means of an event weight, which depends on both, acceptance and rejection probabilities in the parton-shower evolution. In this appendix, we describe a method to incorporate an enhancement, which is constant over the emission phase space. Our derivation is based on the applicability of the veto algorithm, cf. e.g. [26].

Let t be the parton-shower evolution variable and $f(t)$ the splitting kernel $\mathcal{K}$, integrated over the splitting variable z.[3] The differential probability for generating a branching at scale t, when starting from an upper evolution scale t' is then given by

$$\mathcal{P}(t, t') = f(t)\exp\left\{-\int_t^{t'} d\bar{t} f(\bar{t})\right\}. \quad \text{(B1)}$$

A new scale t is therefore found as

[3]For simplicity, we assume that only one splitting function exists, i.e. that there is no flavor change of the splitter during the evolution. The extension to flavor changing splittings is straightforward, but it would unnecessarily complicate the notation at this point.

$$t = F^{-1}[F(t') + \log R] \quad \text{where } F(t) = \int^{t} dt f(t), \tag{B2}$$

and where R is a random number between zero and one. The key point of the veto algorithm is, that even if the integral $F(t)$ is unknown, one can still generate events according to $\mathcal{P}$ using an overestimate $g(t) \geq f(t)$ with a known integral $G(t)$. First, a value t is generated as $t = G^{-1}[G(t') + \log R]$. Second, the value is accepted with probability $f(t)/g(t)$. A splitting at t with n intermediate rejections is then produced with differential probability

$$\begin{aligned}\mathcal{P}_n(t, t') = \frac{f(t)}{g(t)} g(t) \exp\left\{-\int_t^{t_1} d\bar{t} g(\bar{t})\right\} \\ \times \prod_{i=1}^{n}\left[\int_{t_{i-1}}^{t_{i+1}} dt_i \left(1 - \frac{f(t_i)}{g(t_i)}\right) g(t_i) \right. \\ \left. \times \exp\left\{-\int_{t_i}^{t_{i+1}} d\bar{t} g(\bar{t})\right\}\right],\end{aligned} \tag{B3}$$

where $t_{n+1} = t'$ and $t_0 = t$. The nested integrals in Eq. (B3) can be disentangled, and summing over n leads to the exponentiation of the factor $g(t) - f(t)$, such that Eq. (B1) is reproduced [26].

Our purpose is to introduce an additional overestimate $h(t) = Cg(t)$, where C is a constant. The additional weight $g(t)/h(t) = 1/C$ is then applied analytically rather than using a hit-or-miss method. This leads to the following expression for the differential probability to generate an emission at t with n rejections between t and t'

$$\begin{aligned}\mathcal{P}_n(t, t') = \frac{f(t)}{g(t)} h(t) \exp\left\{-\int_t^{t_1} d\bar{t} h(\bar{t})\right\} \\ \times \prod_{i=1}^{n}\left[\int_{t_{i-1}}^{t_{i+1}} dt_i \left(1 - \frac{f(t_i)}{g(t_i)}\right) h(t_i) \right. \\ \left. \times \exp\left\{-\int_{t_i}^{t_{i+1}} d\bar{t} h(\bar{t})\right\}\right] \frac{1}{C} \prod_{i=1}^{n} \frac{g(t_i) - f(t_i)/C}{g(t_i) - f(t_i)}.\end{aligned} \tag{B4}$$

The factor in the second line of Eq. (B4) gives the analytic weight associated with this event, where the term $1/C$ is due to the acceptance of the emission with probability $f(t)/h(t)$. The product, which is needed for an exponentiation of $h(t) - f(t)$ instead of $g(t) - f(t)$, runs over all correction weights for rejected steps.

APPENDIX C: MONTE CARLO SETUP

In this appendix, we describe the details of the Monte Carlo setup used to generate the results in this publication. We employ the SHERPA [36] framework, which is a multipurpose Monte Carlo event generator for collider experiments.

The matrix-element generator COMIX [44] is used to produce parton-level events for the following processes:

$$\begin{aligned} &e^+e^- \text{ collisions (Sec. 4.1)}, \qquad e^+e^- \to rr + Nr, \\ &N \leq N_{\max}, \qquad p\bar{p} \text{ collisions (Sec. 4.2, 4.3)}, \\ &p\bar{p} \to rr + Nr, \qquad N \leq N_{\max}. \end{aligned}$$

The "resummed" container r implements the democratic treatment of photon and parton radiation, i.e. it contains the light quarks d, u, s, c, and b as well as gluons and photons. In addition to all automatically generated tree-level amplitudes, the loop-induced process $gg \to \gamma\gamma$ [17] has been implemented.

As a parton shower, we employ the CSS [30] module which in case of $N_{\max} > 0$ is merged to the matrix-element emissions above $Q_{\text{cut}} = 10$ GeV through the algorithm described in [29]. Unless stated otherwise, we employ the parton-shower kinematics described in Appendix A. All QED splitting functions are included. The shower cutoff has been left at the default value of $p_\perp^{\min} = 1$ GeV for the LEP runs and has been switched to $p_\perp^{\min} = 2$ GeV for the Tevatron runs purely for efficiency reasons.

The PDF set employed for $p\bar{p}$ runs is CTEQ 6L [45], which defines the corresponding α_s parametrization in hadron collisions. All other generator parameters are left at the default values of the Monte Carlo programs, since none of them is expected to have any impact on the results presented here.

Hadron-level results for the fragmentation function analysis in Sec. IV A are produced using the fragmentation module AHADIC++ [46] and the hadron and τ decay package HADRONS++ [47]. The AHADIC++ default tune to data from the LEP experiments at the Z^0 resonance, obtained using the PROFESSOR [48] framework, has been used. To account for corrections in the ALEPH measurement, the decays of π^0 and η have been disabled. Extra QED radiation in hadron decays is simulated through PHOTONS++ [49]. All Tevatron analyses are presented at the parton level after parton-shower evolution.

Multiple parton interactions have been disabled, because the presented measurements have been corrected for their effects.

[1] V. M. Abazov *et al.* (D0 Collaboration), Phys. Rev. Lett. **101**, 051801 (2008); T. Aaltonen *et al.* (CDF Collaboration), Phys. Rev. Lett. **103**, 061803 (2009); G. Aad *et al.* (ATLAS Collaboration), arXiv:0901.0512; G. L. Bayatian *et al.* (CMS Collaboration), J. Phys. G **34**, 995 (2007); D. L. Rainwater and D. Zeppenfeld, J. High Energy Phys. 12 (1997) 005; S. Abdullin *et al.*, Phys. Lett. B **431**, 410 (1998).

[2] I. Hinchliffe and F. E. Paige, Phys. Rev. D **60**, 095002 (1999); G. F. Giudice, R. Rattazzi, and J. D. Wells, Nucl. Phys. **B544**, 3 (1999); H. Davoudiasl, J. L. Hewett, and T. G. Rizzo, Phys. Rev. D **63**, 075004 (2001); C. Macesanu, C. D. McMullen, and S. Nandi, Phys. Lett. B **546**, 253 (2002).

[3] A. Bhatti *et al.*, Nucl. Instrum. Methods Phys. Res., Sect. A **566**, 375 (2006); B. Abbott *et al.* (D0 Collaboration), Nucl. Instrum. Methods Phys. Res., Sect. A **424**, 352 (1999); I. A. Golutvin *et al.*, Phys. Part. Nucl. Lett. **5**, 447 (2008).

[4] P. Aurenche, R. Baier, M. Fontannaz, J. F. Owens, and M. Werlen, Phys. Rev. D **39**, 3275 (1989); W. Vogelsang and A. Vogt, Nucl. Phys. **B453**, 334 (1995); M. Fontannaz and G. Heinrich, Eur. Phys. J. C **34**, 191 (2004).

[5] C. H. Llewellyn Smith, Phys. Lett. **79B**, 83 (1978).

[6] H. Baer, J. Ohnemus, and J. F. Owens, Phys. Rev. D **42**, 61 (1990).

[7] P. Aurenche, R. Baier, and M. Fontannaz, Phys. Rev. D **42**, 1440 (1990).

[8] E. W. N. Glover and A. G. Morgan, Z. Phys. C **62**, 311 (1994); A. Gehrmann-De Ridder, T. Gehrmann, and E. W. N. Glover, Phys. Lett. B **414**, 354 (1997).A. Gehrmann-De Ridder and E. W. N. Glover, Eur. Phys. J. C **7**, 29 (1999).

[9] S. Frixione, Phys. Lett. B **429**, 369 (1998); S. Frixione and W. Vogelsang, Nucl. Phys. **B568**, 60 (2000).

[10] P. Aurenche, R. Baier, M. Fontannaz, and D. Schiff, Nucl. Phys. **B297**, 661 (1988).

[11] L. E. Gordon and W. Vogelsang, Phys. Rev. D **50**, 1901 (1994).

[12] P. Aurenche, A. Douiri, R. Baier, M. Fontannaz, and D. Schiff, Z. Phys. C **29**, 459 (1985).

[13] B. Bailey, J. F. Owens, and J. Ohnemus, Phys. Rev. D **46**, 2018 (1992).

[14] S. Catani, M. Fontannaz, J. P. Guillet, and E. Pilon, J. High Energy Phys. 05 (2002) 028; P. Aurenche, M. Fontannaz, J.-P. Guillet, E. Pilon, and M. Werlen, Phys. Rev. D **73**, 094007 (2006); Z. Belghobsi *et al.*, Phys. Rev. D **79**, 114024 (2009).

[15] T. Binoth, J. P. Guillet, E. Pilon, and M. Werlen, Eur. Phys. J. C **16**, 311 (2000); Phys. Rev. D **63**, 114016 (2001).

[16] V. Del Duca, F. Maltoni, Z. Nagy, and Z. Trocsanyi, J. High Energy Phys. 04 (2003) 059.

[17] E. L. Berger, E. Braaten, and R. D. Field, Nucl. Phys. **B239**, 52 (1984).

[18] D. de Florian and Z. Kunszt, Phys. Lett. B **460**, 184 (1999); C. Balazs, P. M. Nadolsky, C. Schmidt, and C. P. Yuan, Phys. Lett. B **489**, 157 (2000); T. Binoth, J. P. Guillet, and F. Mahmoudi, J. High Energy Phys. 02 (2004) 057.

[19] C. Balazs, E. L. Berger, S. Mrenna, and C. P. Yuan, Phys. Rev. D **57**, 6934 (1998); C. Balazs, E. L. Berger, P. M. Nadolsky, and C. P. Yuan, Phys. Lett. B **637**, 235 (2006); Phys. Rev. D **76**, 013009 (2007).

[20] N. Kidonakis and J. F. Owens, Phys. Rev. D **61**, 094004 (2000); D. de Florian and W. Vogelsang, Phys. Rev. D **72**, 014014 (2005).

[21] G. Diana, Nucl. Phys. **B824**, 154 (2010).

[22] T. Becher and M. D. Schwartz, arXiv:0911.0681.

[23] D. R. Yennie, S. C. Frautschi, and H. Suura, Ann. Phys. (N.Y.) **13**, 379 (1961).

[24] D. J. Summers, Phys. Rev. D **53**, 2430 (1996).

[25] M. H. Seymour, Z. Phys. C **56**, 161 (1992); **64**, 445 (1994).

[26] T. Sjöstrand, S. Mrenna, and P. Skands, J. High Energy Phys. 05 (2006) 026; Comput. Phys. Commun. **178**, 852 (2008); G. Corcella *et al.*, J. High Energy Phys. 01 (2001) 010; M. Bähr *et al.*, Eur. Phys. J. C **58**, 639 (2008); L. Lönnblad, Comput. Phys. Commun. **71**, 15 (1992).

[27] F. Krauss, A. Schälicke, S. Schumann, and G. Soff, Phys. Rev. D **70**, 114009 (2004); F. Krauss, A. Schälicke, S. Schumann, and G. Soff, Phys. Rev. D **72**, 054017 (2005); T. Gleisberg, F. Krauss, A. Schälicke, S. Schumann, and J.-C. Winter, Phys. Rev. D **72**, 034028 (2005); J. Alwall *et al.*, Eur. Phys. J. C **53**, 473 (2008).

[28] M. L. Mangano, M. Moretti, F. Piccinini, and M. Treccani, J. High Energy Phys. 01 (2007) 013; J. Alwall, S. de Visscher, and F. Maltoni, J. High Energy Phys. 02 (2009) 017; T. Plehn and T. M. P. Tait, J. Phys. G **36**, 075001 (2009).

[29] S. Höche, F. Krauss, S. Schumann, and F. Siegert, J. High Energy Phys. 05 (2009) 053.

[30] S. Schumann and F. Krauss, J. High Energy Phys. 03 (2008) 038.

[31] T. Carli, T. Gehrmann, and S. Höche, arXiv:0912.3715.

[32] S. Catani and M. H. Seymour, Nucl. Phys. **B485**, 291 (1997); S. Catani, S. Dittmaier, M. H. Seymour, and Z. Trocsanyi, Nucl. Phys. **B627**, 189 (2002).

[33] S. Plätzer and S. Gieseke, arXiv:0909.5593.

[34] A. D. Martin, R. G. Roberts, W. J. Stirling, and R. S. Thorne, Eur. Phys. J. C **39**, 155 (2005).

[35] S. Catani, Y. L. Dokshitzer, and B. R. Webber, Phys. Lett. B **285**, 291 (1992); S. Catani, Y. L. Dokshitzer, M. H. Seymour, and B. R. Webber, Nucl. Phys. **B406**, 187 (1993).

[36] T. Gleisberg, S. Höche, F. Krauss, A. Schälicke, S. Schumann, and J. Winter, J. High Energy Phys. 02 (2004) 056.T. Gleisberg, S. Höche, F. Krauss, M. Schönherr, S. Schumann, F. Siegert, and J. Winter, J. High Energy Phys. 02 (2009) 007.

[37] D. Buskulic *et al.*, Z. Phys. C **69**, 365 (1996).

[38] T. Aaltonen (CDF Collaboration), Phys. Rev. D **80**, 111106 (2009).

[39] V. M. Abazov *et al.* (D0 Collaboration), Phys. Lett. B **639**, 151 (2006).

[40] D. E. Acosta *et al.* (CDF Collaboration), Phys. Rev. Lett. **95**, 022003 (2005).

[41] W. Chen, Ph.D. thesis, SUNY Stony Brook, 1997.

[42] M. A. G. Aivazis, J. C. Collins, F. I. Olness, and W.-K. Tung, Phys. Rev. D **50**, 3102 (1994).

[43] R. Pittau, Comput. Phys. Commun. **104**, 23 (1997); **111**, 48 (1998).

[44] T. Gleisberg and S. Höche, J. High Energy Phys. 12 (2008) 039.

[45] J. Pumplin, D. R. Stump, J. Huston, H. L. Lai, P. Nadolsky, and W. K. Tung, J. High Energy Phys. 07 (2002) 012.
[46] J.-C. Winter, F. Krauss, and G. Soff, Eur. Phys. J. C **36**, 381 (2004); ''SHERPA's new hadronisation model'' (unpublished).
[47] F. Krauss, T. Laubrich, and F. Siegert, ''Simulation of hadron decays in SHERPA'' (unpublished).
[48] A. Buckley, H. Hoeth, H. Lacker, H. Schulz, and J. E. von Seggern, Eur. Phys. J. C **65**, 331 (2010).
[49] M. Schönherr and F. Krauss, J. High Energy Phys. 12 (2008) 018.